HHS Public Access

Author manuscript

Nat Neurosci. Author manuscript; available in PMC 2009 November 01.

Published in final edited form as:

Nat Neurosci. 2009 May ; 12(5): 585–592. doi:10.1038/nn.2302.

BK channels modulate pre- and postsynaptic signaling at reciprocal synapses in retina

William N. Grimes[1,2], **Wei Li**[3], **Andrés E. Chávez**[1,4], and **Jeffrey S. Diamond**[1]

[1]Synaptic Physiology Section, National Institute of Neurological Disorders and Stroke

[2]University of Maryland/NIH Biophysics Graduate Partnership Program

[3]Unit on Retinal Neurophysiology, National Eye Institute

Abstract

In the mammalian retina, A17 amacrine cells provide reciprocal inhibitory feedback to rod bipolar cells, thereby shaping the time course of visual signaling *in vivo*. Previous results indicate that A17 feedback can be triggered by Ca^{2+} influx through Ca^{2+} permeable AMPARs and can occur independently of voltage-gated Ca^{2+} (Ca_V) channels, whose presence and functional role in A17 dendrites have not been explored. Here, we combine electrophysiology, calcium imaging and immunohistochemistry to show that L-type Ca_V channels in rat A17 amacrine cells are located at the sites of reciprocal synaptic feedback, but their contribution to GABA release is diminished by large-conductance Ca^{2+}-activated potassium (BK) channels, which suppress postsynaptic depolarization in A17s and limit Ca_V channel activation. We also show that BK channels, by limiting GABA release from A17s, regulate the flow of excitatory synaptic transmission through the rod pathway.

Introduction

Rod bipolar cell (RBC)/ AII amacrine cell/ A17 amacrine cell dyad synapses limit the gain of the rod pathway in the mammalian retina1. RBCs make excitatory (glutamatergic) ribbon-type synapses onto AII and A17 amacrine cell processes; in return, A17s make reciprocal inhibitory (GABAergic) synapses back onto RBC terminals2–4 that sharpen the time course of rod-driven visual signals *in vivo*5. Reciprocal GABA release from A17s can be triggered directly by Ca^{2+} influx through Ca^{2+}-permeable AMPA receptors (CP-AMPARs) and consequent calcium-induced Ca^{2+} release (CICR) from intracellular stores, resulting in the activation of GABA receptors (GABARs) on RBC terminals6. Those experiments indicated that evoked transmitter release from A17s can occur independently of voltage-gated calcium

Correspondence: Jeffrey S. Diamond, Ph.D., Synaptic Physiology Section, National Institute of Neurological Disorders and Stroke, National Institutes of Health, 35 Convent Drive, Bethesda, MD 20892–3701, Phone: (301) 435–1896, FAX: (301) 435–1895, Email: diamondj@ninds.nih.gov.

[4]Present Address: Department of Neuroscience, Albert Einstein College of Medicine

Author Contributions

W.N.G. conducted the electrophysiological experiments; W.L. conducted the immunohistochemistry experiments; A.E.C. conducted preliminary electrophysiological experiments contributing to the formulation of the project; W.N.G., A.E.C. and J.S.D. designed the experiments; W.N.G. and J.S.D. wrote the manuscript.

(Ca_v) channels. Although indirect evidence for Ca_v channels in A17s has been reported6,7, the type and location of these channels is unknown. Even if Ca_v channels were localized to the bouton-like varicosities where reciprocal GABA feedback occurs, it is possible that their contribution to GABA release could be prevented by biochemical compartmentalization, or perhaps another conductance that could counteract synaptic depolarization and limit Ca_v channel activation.

Recent studies indicate that Ca^{2+}-activated potassium (K_{Ca}) channels can regulate synaptic transmission and spike frequency8–16. K_{Ca} channel nomenclature refers specifically to single channel conductance (γ), but other biophysical properties also differ substantially. Small-conductance K_{Ca} (SK) channels (γ = 9–10 pS) are activated solely by intracellular Ca^{2+} levels, whereas large (big)-conductance K_{Ca} (BK) channels (γ = 100–270 pS) are activated both by voltage and Ca^{2+} and can inactivate rapidly if auxiliary β subunits are present17–19. SK channels can be activated by rises in intracellular Ca^{2+} attributed to influx through Ca_v channels, release from intracellular stores, or synaptic activation of NMDARs. This coupling has direct consequences for synaptic plasticity, calcium spikes, action potential shape and firing frequency in several areas of the CNS8,12. The impact of BK channel activation on synaptic and network physiology is less well understood. The voltage-dependence of BK channels shifts towards negative potentials when intracellular Ca^{2+} levels increase20,21, enabling the channels to affect action potential repolarization and spontaneous firing22,23.

Here we show that rapidly-inactivating BK channels modulate both excitatory and inhibitory synaptic transmission at the RBC-A17 reciprocal feedback synapse in rat retina. Experiments employing a combination of electrophysiology, pharmacology, two-photon Ca^{2+} imaging and immunohistochemistry approaches indicate that BK channels are colocalized with L-type Ca_v channels, intracellular calcium stores and AMPAR-mediated synaptic inputs within individual synaptic varicosities along A17 dendrites. Blocking BK channels in A17s potentiates EPSPs and results in increased reciprocal GABA release and increased suppression of feed forward signaling at the rod bipolar cell dyad. These experiments illustrate a novel example of subcellular mechanisms within an interneuron working in concert to regulate information flow through an excitatory network.

Results

Ca_v channels are located in A17 synaptic varicosities

Although previous work suggests that A17 membranes exhibit voltage-activated Ca^{2+}-permeability7, GABA release from A17s can occur independently of Ca_v channels6. One possible explanation for this apparent paradox is that Ca_v channels may not be located in the A17 varicosities where GABA feedback occurs. To test this idea, we made Ca^{2+} fluorescence measurements from the specialized synaptic compartments along A17 dendrites that have been shown to be reciprocally connected to RBC ribbon synapses3,24. Whole cell recordings were made from amacrine cells with relatively large somas (diameter ~ 10 μm) adjacent to the inner plexiform layer (IPL). Fluo-5F (200 μM) and Alexa 594 (40 μM) were included in the patch pipette to monitor intracellular Ca^{2+} and cell morphology, respectively. A17 amacrine cells (Fig. 1a and Fig 3a) were identified by the combination of

several features: 1) multiple non-branching appendages extending from the soma into sublamina 5 of the IPL, where A17s receive synaptic input from RBCs; 2) small varicosities along the length of the dendrites (at ~15–20 μm intervals24); and 3) input resistance in the range of 150–350 MΩ (245 ± 75 MΩ, n = 159). After an approximately 30-minute dialysis period, we electrically stimulated bipolar cells in the outer plexiform layer (OPL) and searched for time-locked fluorescence transients in individual A17 varicosities. Synaptically-evoked Ca^{2+} responses under voltage-clamp were difficult to locate due to the small size and low density of varicosities, so cyclothiazide (50 μM) was included in the bath solution to enhance AMPAR affinity for glutamate and remove desensitization25. Under these conditions, synaptically-evoked fluorescence transients could be observed in a small subset of varicosities (Fig. 1b *middle*). Varicosities adjacent to the responding varicosity along a single dendrite were typically unresponsive to synaptic stimulation (not shown), suggesting that the Ca^{2+} response was predominantly a result of synaptic activation of the responding varicosity. If a synaptically evoked Ca^{2+} signal was observed, we then tested the varicosity for a voltage-activated Ca^{2+} response by applying a depolarizing voltage step through the somatic recording electrode (−70 mV to −10 mV, 100 ms; Fig. 1b *right*). In almost every case, a varicosity that responded to synaptic stimulation also responded to voltage steps (35 of 36 varicosities, n = 23 different cells; Fig. 1f) indicating that Ca_v channels are colocalized with synaptic inputs at individual feedback varicosities. These signals arose via distinct mechanisms: application of the AMPAR antagonist NBQX (10 μM) blocked synaptically evoked currents (to 0.4 ± 0.8% of control, n = 5; P = 0.0052; Fig. 1c,d *left*, e *left*) and fluorescence (to 0.5 ± 6.9% of control, n = 5, P = 0.0097; Fig. 1b *middle*,c, e *left*) but not step evoked currents (101 ± 14% of control, n = 5, P = 0.62; Fig. 1c,d *right*, e *right*) or fluorescence (99 ± 44% of control, n = 5, P = 0.29; Fig. 1b *right*, c, e *right*).

To identify the primary subtype and location of Ca_v channels in A17s, we examined the voltage-dependence and pharmacology of Ca_v signals with electrophysiological and imaging techniques. Families of 100 ms voltage steps (−70 mV to +50 mV, 20 mV increments) revealed sustained inward currents that were sensitive to isradipine (−38 ± 16 pA block at −10 mV, n = 17, P < 0.0001; Fig. 2a), indicating the presence of L-type Ca_v channels. Consistent with blockade of inward Ca^{2+} current, isradipine strongly reduced voltage step-evoked fluorescence transients in the cell bodies (to 34 ± 11% of control, n = 6, P = 0.004) and varicosities (to 23 ± 13% of control, n = 5, P = 0.006) of A17s (Fig. 2c). Voltage-activated fluorescence transients were observed in all varicosities tested within 100 μm of the soma as well as in all somata.

Both CP-AMPARs and CICR have been shown to trigger neurotransmitter release from A17s6. To examine the contributions of CICR to voltage-activated Ca^{2+} signaling in A17 varicosities, excitatory and inhibitory synaptic transmission was pharmacologically blocked and voltage-activated (−70 mV to −20 mV, 100 ms) single varicosity fluorescence (Fig. 3b, white box in Fig. 3a) was observed under control conditions and in the presence of thapsigargin (1 μM), which depletes internal Ca^{2+} stores by blocking SERCA pumps26. Depletion of intracellular stores did not reduce the recorded Ca^{2+} current (99 ± 16% of control at −20 mV, n = 5, P = 0.57; Fig. 3d,e) but did significantly reduce the observed

fluorescence (to 59 ± 19% of control at −20 mV, n = 5, P = 0.0091; Fig. 3c,d), indicating that Ca^{2+} influx through Ca_v channels triggers CICR within varicosities.

BK channels are localized to A17 feedback varicosities

If Ca_v channels are located in synaptic varicosities, why don't they contribute to GABAergic feedback? One possibility is that some other mechanism limits synaptic depolarization and, therefore, Ca_v channel activation. Spontaneous potassium currents have previously been observed in acutely dissociated amacrine cells from tiger salamander27. These transient currents were sensitive to iberiotoxin, a component of scorpion venom that selectively antagonizes BK channels. A synaptic event causing a coincident local depolarization and increased cytosolic Ca^{2+}, via Ca^{2+} influx through CP-AMPARs, Ca_v channels and/or subsequent CICR, could activate a hyperpolarizing BK current to counteract AMPAR-mediated depolarization and rapidly suppress Ca_v channel activation.

To test for functional BK channels in A17s, voltage clamp recordings were made from A17 amacrine cells in slice with K^+-based internal solutions; A-type K_v channels were blocked with 4-AP (4 mM). Depolarizing voltage steps (from −90 mV to −30 mV for 200 ms) elicited a sustained, inward Ca_v channel-mediated current and a transient, outward current that was completely blocked by iberiotoxin (100 nM; to 2 ± 9% of control, P = 0.011, n = 5; Fig. 4a), indicating the functional presence of BK channels in A17s. Although both the current through slowly inactivating L-type Ca_v channels and the observed (highly buffered) voltage-dependent calcium signals decayed on the order of hundreds of milliseconds (see Fig. 2), the transient BK currents decayed much more quickly (τ = 4.4 ± 1.3 ms, n = 5), suggesting that BK channels in A17s inactivate rapidly. Pairs of steps (−90 mV to −30 mV, 40 ms) at varying interstep intervals indicated that the Ca_v channel-coupled BK pathway recovers from inactivation with a time constant of 23.6 ± 4.7 ms (n = 5; Fig 4b).

We next tested whether BK channels can be activated by Ca^{2+} influx through L-type Ca_v channels. Application of isradipine (10 μM) strongly reduced the transient outward current (to 13 ± 11% of control, n = 5, P = 0.035; Fig 4c) indicating that L-type Ca_v channel activation can trigger BK currents. The coupling between Ca_v channel-mediated Ca^{2+} influx and BK channel activation is not enhanced by CICR, as depleting intracellular stores with thapsigargin (1 μM) only slightly reduced BK currents elicited by voltage steps to −30 mV (to 92 ± 11% of control, n = 5, P = 0.063; not shown).

As a further test for BK expression, A17s were filled through the patch pipette with neurobiotin (50 mM) and slices were incubated in streptavidin (green, binds neurobiotin) and antibodies to PKCα (blue, labels RBCs) and BK channels (red) or the auxiliary subunit responsible for BK inactivation, β2 (red). BK immunoreactivity was evident throughout the IPL and was strongest in sublamina 5, which contains the RBC terminals and A17 varicosities (Fig. 4d). Higher magnification of sublamina 5 revealed clusters of fluorescent puncta surrounding RBC terminals (slice: Fig. 4e; whole-mount: Fig. 4g). In 89 A17 varicosities apposed to RBC terminals imaged in 5 different slices, 72 (81%) were colocalized with BK puncta (Fig. 4e). Consistent with the physiological observation that A17 BK channels inactivate rapidly (Fig. 4a, b), β2 subunit immunoreactivity displayed a

similar pattern to that of BK antibodies, with individual puncta colocalized with A17 varicosities (Fig. 4f) and surrounding RBC terminals (whole mount: Fig. 4h).

Despite the strong agreement between the physiological and anatomical data, it is difficult to exclude the possibility that some immunoreactivity in sublamina 5 may reflect BK channel expression in postsynaptic AII amacrine cell membranes. Consistent with this possibility, iberiotoxin-sensitive BK currents, elicited by step depolarization, also were observed in AII amacrine cells and exhibited a mix of inactivating and non-inactivating components (inactivating component: 68 ± 8 % of the total amplitude; n = 5; data not shown). These results indicate that Ca_v channel-mediated Ca^{2+} influx can activate BK channels in AII amacrine cells. Ca^{2+} imaging studies indicate, however, that step depolarization of AII somata elicits Ca^{2+} influx in lobular appendages in the outer IPL but not in processes postsynaptic to RBC terminals28 (unpublished observations). Therefore, although the (step-evoked) BK currents that we record in AII amacrine cells probably do not originate in the postsynaptic membrane near RBC ribbon synapses, BK channels may nonethesless be expressed there, perhaps working in concert with CP-AMPARs4,29.

BK channels suppress synaptic depolarization

If BK channels in A17 amacrine cells were activated during synaptic transmission, they may counteract AMPAR-induced depolarization and reduce the amplitude of EPSPs. To test this hypothesis, we recorded from A17s in the current-clamp configuration (K^+-based internal) with inhibition blocked and elicited EPSPs by electrical stimulation of afferent bipolar cells in the outer plexiform layer (OPL). Blocking BK channels with iberiotoxin potentiated EPSPs (141 ± 30% of control, n = 6, P = 0.049; Fig. 5a), suggesting that synaptically-activated BK channels limit synaptic depolarization.

Iberiotoxin did not affect EPSCs recorded under voltage clamp (with Cs-based internal solution, 97 ± 8% of control; n = 5; P = 0.18; Fig. 5b,c) indicating that the drug affects neither transmitter release from RBCs nor AMPARs on A17s. These results indicate that BK currents counterbalance synaptic AMPAR-mediated EPSCs in A17 synaptic varicosities, an interaction that may be optimized by the kinetic similarities between the two currents (EPSC τ_{decay} = 3.2 ± 1.6 ± ms, n = 5; BK current $\tau_{inactivation}$ = 4.4 ± 1.3 ms, n = 5; Fig. 5d,e).

BK channels limit GABA release from A17s

To what extent do Ca_v channels and BK channels contribute to feedback inhibition onto RBC terminals? GABA release from A17s can be measured in RBCs by puffing glutamate onto A17 dendrites and recording IPSCs in voltage-clamped RBCs6. Here we elicited IPSCs in RBCs (V_{hold} = 0 mV) with brief glutamate puffs (50 and 500 μM, 25 ms) in the presence of TTX (1μM) and strychnine (1 μM) to isolate A17-mediated feedback. In agreement with Chavez *et al.* (2006), application of Cd^{2+} (200 μM), a Ca_v channel pore blocker, only slightly reduced the IPSCs evoked by 50 μM glutamate (91 ± 5% of control, n = 6, P = 0.012; Fig. 6a). Application of iberiotoxin (100 nM) significantly enhanced IPSCs evoked by 50 μM glutamate (117 ± 11% of control, n = 6, P = 0.022), indicating that BK channels limit GABA release from A17s. The enhancement caused by iberiotoxin was essentially removed by Cd^{2+} (97 ± 12% of control, n = 6, P = 0.33; Fig. 6b), suggesting that BK

channels prevent Ca_v channel contributions to GABA release elicited by 50 μM glutamate. Apamin (100 nM), an SK channel antagonist, had no significant affect on IPSCs (97 ± 10% of control, n = 6, P = 0.39). If blocking BK channels reveals a Ca_v channel dependent enhancement of reciprocal inhibition, one might predict that stronger activation of dendritic AMPARs could overwhelm BK channels and recruit Ca_v channels to trigger GABA release under basal conditions, thus exposing a voltage-dependent component of GABA release. Accordingly, puffing a higher concentration of glutamate (500 μM) onto A17 dendrites elicited larger IPSCs (500 μM puff: 28 ± 11 pA, n = 14; 50 μM puff: 14 ± 4 pA, n = 12; unpaired t-test P = 0.0005) that were significantly reduced by Cd^{2+} (48 ± 19% of control, n = 9, P = 0.0029; Fig. 6c). Application of iberiotoxin enhanced these IPSCs (118 ± 6% of control, n = 5, P = 0.0038) and, again, Cd^{2+} blocked a significant proportion of the response (to 43 ± 10% of iberiotoxin, n = 5, P = 0.012; Fig. 6d), suggesting that BK channels continue to suppress Ca_v channel activation even under stronger stimulus conditions. These results demonstrate that BK channels limit GABAergic transmission from A17s by reducing Ca^{2+} influx through Ca_v channels and thus suppressing neurotransmitter release.

The experiments presented thus far show that multiple mechanisms can trigger and modulate reciprocal GABA release from A17s and that these mechanisms are activated differentially depending on the strength of stimulation. To test this model further, cyclothiazide (50 μM) was applied to enhance AMPAR affinity for glutamate and to remove desensitization, thereby enhancing A17 responsivity. Cyclothiazide strongly increased EPSPs in A17s (amplitude: 309 ± 52% of control, n = 5, P = 0.0004; Fig. 7a,b), demonstrating that enhancing AMPAR efficacy strongly potentiates the postsynaptic response. Application of cyclothiazide should increase IPSCs elicited by weak presynaptic activation (50 μM glutamate puff; 25 ms) by increasing the total inward charge transfer and potentially overwhelming the rapidly inactivating inhibitory BK conductance. Consistent with this prediction, cyclothiazide increased IPSC amplitude (153 ± 44% of control, n = 15, P = 0.00099); the enhanced IPSCs were significantly blocked by Cd^{2+} (to 72 ± 14% of cyclothiazide alone, n = 7, P = 0.011; Fig. 7c,d), suggesting that increasing the responsivity of AMPARs enables access to Ca_v channel-dependent feedback mechanisms. 5,7-DHT (50 μM), a toxic serotonin analog that ablates indoleamine-accumulating cells such as A17s5,6, abolished the cyclothiazide-enhanced IPSCs (to 2 ± 3% of cyclothiazide alone, n = 4, P = 0.0026; Fig. 7d), indicating that the enhanced inhibition was entirely attributed to A17s.

BK channels regulate feedforward rod pathway signaling

The results presented above indicate that BK channels limit synaptic depolarization and evoked transmitter release from A17 amacrine cells. How do these effects influence the evoked synaptic output of RBCs? Blocking BK channels enhances feedback inhibition onto RBCs from A17s (Fig. 6), suggesting that application of iberiotoxin should decrease evoked glutamate release from RBCs. The effects of iberiotoxin on light-evoked responses in the rod pathway would be complicated by the complex effects of BK channels on transmitter release from rod photoreceptors16. To avoid this problem, we electrically stimulated bipolar cells with an electrode positioned in the OPL and monitored RBC synaptic output by recording EPSCs in AII amacrine cells.

By systematically changing the duration of the current pulse delivered through the electrode (see Methods), synaptic stimulation strength was varied to span the entire dynamic range of RBC output (Fig. 8a). Consistent with the above prediction, iberiotoxin significantly reduced the dyad output for stimulus durations greater than 100 μs (e.g., to 46 ± 22 % control for 200 μs stim., n = 8, P = 0.0009; Fig. 8a,c). This reduction was almost completely eliminated in the presence of 5,7,-DHT (e.g., to 104 ± 35 % of DHT alone for 200 μs stim., n = 8, P = 0.72; Fig. 8b,c), indicating that iberiotoxin's effects were due primarily to actions of BK channels in A7 amacrine cells. Iberiotoxin caused a larger reduction of responses elicited by weaker stimulation (200 μs stim: 46 ± 22 % of control vs. 600 μs stim: 66 ± 5 % of control, n = 8, P = 0.025; Fig. 8c), confirming that BK channels are most effective at limiting Ca_V channel activation and GABA release in response to small synaptic depolarizations.

Discussion

The results presented here demonstrate that BK channels can modulate both excitatory and inhibitory synaptic transmission via suppression of glutamatergic synaptic depolarizations and the consequent Ca_V channel activation. The impact of this regulation was illustrated by experiments showing that BK channels regulate feedforward signaling in the intact rod circuitry. Exhibiting interactions that are functionally analogous to those between NMDARs and SK channels in the hippocampus and lateral amygdala8,12, BK channels in A17 dendritic varicosities are coupled to CP-AMPAR-mediated synaptic responses. BK channels are known to form macromolecular complexes with L-, N- and P/Q-type Ca_V channels20; in A17 amacrine cells, BK conductances not only can be triggered directly by L-type Ca_V channel activation but also reduce Ca_V channel contributions to GABA release. Glutamate puff-evoked IPSC experiments demonstrate that Ca_V channels enhance GABA release only when A17 dendrites are more strongly activated and that BK channels regulate the extent of this voltage-dependent signaling (Fig. 6). Vesicular glutamate release from RBC ribbon synapses is proportional to membrane depolarization4, thereby providing a discretized yet extended range of inputs to A17 varicosities. Based on these findings, together with previous results from our laboratory6, we argue that L-type Ca_V channels, BK channels, CP-AMPARs and CICR within single varicosities (Supplementary Fig. 1) work in concert to provide an extended range of reciprocal feedback inhibition that is membrane potential dependent or independent, depending on the strength of feedforward signaling.

BK channels dynamically regulate reciprocal inhibition

In many central neurons, non-inactivating SK channels mediate an inhibitory conductance that is well suited to suppress long lasting NMDAR-mediated responses8,11,12. Here we present an analogous scenario in which rapidly inactivating BK channels counter similarly fast AMPAR-mediated depolarizations (Fig. 5). This close temporal match may enable BK channels to efficiently suppress EPSPs during single synaptic events within individual varicosities. Importantly, this suppression persists over a very broad time scale, as BK channels also limit Ca_V channel activation during puff-evoked responses (Fig. 6) that are slower than light-evoked signaling in the rod pathway30. Together, these results indicate that, although BK channel-mediated regulation at individual sites of feedback likely depends

on fast interactions between colocalized conductances with rapid kinetics, it also modulates reciprocal inhibition within the retinal circuitry on longer, more physiologically relevant time scales.

Our immunohistochemistry results and inactivation/recovery measurements suggest that fast BK inactivation in A17s is due to the presence of β2 auxiliary subunits. Each β2 subunit has a charged N-terminus that inactivates BK channels by blocking the pore17. The presence of β2 subunits also shifts the voltage dependence of BK activation at a particular intracellular Ca^{2+} concentration towards more negative, physiological potentials in a stoichiometry-dependent (β:α) manner32. The observed rapid inactivation of BK channels by auxiliary β2 subunits suggests a potentially activity-dependent role for these channels in regulating feedback inhibition. We propose a physiological model in which BK channels dynamically regulate A17 physiology: When spontaneous release from RBCs is relatively infrequent (under dim light conditions1,33), highly available BK channels suppress synaptic depolarizations (elicited by weak light stimuli) within stimulated varicosities and the consequent electrotonic spread to neighboring varicosities on the same dendrite. Under these conditions, synapse-specific reciprocal inhibition is triggered via Ca^{2+} influx through CP-AMPARs (and possibly amplification of local calcium signals by CICR), but BK channels limit Ca_v channel activation and, therefore, the absolute amplitude of local reciprocal inhibition. As mean light levels increase, spontaneous synaptic input (i.e., noise) increases, depolarizing A17 dendrites and inactivating BK channels. With BK channels inactivated, excitatory signals would elicit stronger synaptic depolarizations within the stimulated varicosity and in neighboring varicosities, therefore increasing Ca_v channel activation, GABA release, and the spatial extent of “surround” feedback inhibition.

BK channels in A17s regulate the gain of RBC synapses

The recordings of EPSCs in AII amacrine cells (Fig. 8) begin to provide a framework for understanding the physiological role of BK-modulated reciprocal inhibition in the context of feedforward information flow in the rod pathway. BK channels appear to enhance the amplitude of feedforward excitatory signaling, presumably by limiting Ca_v channel activation and reciprocal inhibition within A17 amacrine cell varicosities. This modulation of feedforward transmission was significantly greater for smaller signals (Fig. 8c), indicating that BK and Ca_v channels contribute to a varying extent over the range of stimulus strengths, consistent with the feedback IPSC experiments (Fig. 6).

When considering the low signal-to-noise ratio under dim light conditions, it is not surprising that an inhibitory feedback mechanism, capable of suppressing transient responses, should be minimized. Furthermore, the high axial resistance between varicosities3,34 and the reduced EPSPs would suggest that BK channels could modulate the extent of interactions between neighboring dyad microcircuits along A17 dendrites. Further experiments and modeling efforts will be necessary to determine the electrotonic structure of A17 and how this interneuron dynamically regulates spatial processing in the inner retina.

Methods

Electrophysiology

Experiments were conducted at room temperature (22–25° C) using light-adapted retinal slices (210 μm thick) prepared from Sprague-Dawley rats (P17–21), as approved by the NINDS Animal Care and Use Committee and as previously described4,6. Rat retinas were isolated in artificial cerebrospinal fluid (ACSF) containing (in mM): 119 NaCl, 26 $NaHCO_3$, 1.25 Na_2HPO_4, 2.5 KCl, 2.5 $CaCl_2$, 1.5 $MgSO_4$, 10 glucose, 2 Na-pyruvate, 4 Na-lactate and equilibrated with 95% O_2/5% CO_2. For synaptic experiments, unless otherwise noted, ACSF was supplemented with the group III mGluR agonist L-AP4 (10 μM) and strychnine (1 μM) and tetrodotoxin (TTX, 1 μM) to block glycine receptors and voltage-gated sodium channels, respectively. For all non-synaptic experiments (ie. voltage-dependent responses), ACSF was supplemented with TTX (1 μM) and the AMPAR antagonist, NBQX (10 μM). For clearer observation of voltage-step activated BK currents (Fig. 4), 4-AP (4 mM) was included in the bath solution to block A-type potassium channels. Drugs were purchased from Sigma or Tocris (St. Louis, MO) with the exception of TTX (Alamone Labs, Jerusalem, Israel). All fluorescent dyes were purchased from Molecular Probes (Eugene, OR).

Whole-cell voltage-clamp recordings were made from RBCs using pipettes (~7–9 MΩ) containing (in mM): 100 Cs methanesulfonate, 20 TEA-Cl, 10 HEPES, 1.5 BAPTA, 10 Na phosphocreatine, 4 Mg-ATP, 0.4 Na-GTP, 10 L-glutamic acid and 0.02 Alexa-488 hydrazide (pH 7.4). RBC access resistance was 25–50 MΩ and was left uncompensated. Unless otherwise noted, whole-cell voltage-clamp recordings were made from A17s and AIIs using pipettes (~5–6 MΩ) containing (in mM): 100 Cs methanesulfonate, 20 TEA-Cl, 10 HEPES, 10 EGTA, 10 Na phosphocreatine, 4Mg-ATP, 0.4 Na-GTP and 0.04 Alexa-594 hydrazide (pH 7.4). Potassium-based internal for amacrine cells contained (in mM): 100 K methanesulfonate, 20 TEA-Cl, 10 HEPES, 2 EGTA, 10 Na phosphocreatine, 4Mg-ATP, 0.4 Na-GTP and 0.04 Alexa-594 hydrazide (pH 7.4). A17 and AII access resistance was ≤30 MΩ and was left uncompensated. Recordings were made using an Axopatch 1D amplifier (Axon Instruments, Foster City, CA) which was interfaced with an Instrutech ITC-18 analog-to-digital board and controlled by custom software written for Igor Pro (Wavemetrics, Lake Oswego, OR). Synaptic responses recorded in A17 were elicited by electrical stimulation of bipolar cells in the OPL (~10–30 μA for 200–300 μs; Getting Instruments, Iowa City, IA). For experiments designed to examine the range of dyad outputs (described in Figure 8) the stimulus amplitude was set such that the maximal stimulus duration (600 μs) provided a nearly saturating response in the AII amacrine cell. Synaptic responses recorded in RBCs were elicited by focal puff application of glutamate (50 or 500 μM for 25 ms) in sublamina 5 of the IPL using a Picospritzer (General Valve, Fairfield, NJ). All current responses were collected at 12, 20 or 25 s intervals, low-pass filtered at 5 kHz and digitized at 10 kHz. Voltage steps were leak-subtracted using the p/4 subtraction protocol. Electrophysiology data was analyzed using Igor Pro and Excel (Microsoft, Seattle, WA). Step-evoked currents and the raw fluorescence example in Fig. 3c were smoothed using the built-in Igor binomial smoothing function to emphasize kinetics of the responses.

Pooled data in Fig. 8a,b were fit with a sigmoid using the built in Igor Pro fitting procedures to make the trends more visually apparent to the reader.

Statistical Analysis

Paired, two-tailed *t* tests (unless otherwise noted) were used to compare data sets and significance was determined as $P < 0.05$ (*), $P < 0.01$ (**), or $P < 0.001$ (***). Unless otherwise indicated, data are presented as mean ± SD and illustrated traces are averages of 5–10 responses.

Two-photon Ca^{2+} imaging

Ca^{2+} responses were observed by replacing EGTA with Fluo-5F (200 μM) in the described A17 internal solution and acquired using a modified Zeiss LSM 510 with Multi-Time acquisition software. The excitation source consisted of a computer-controlled Chameleon infrared laser (λ = 810 nm; Coherent, Santa Clara, CA) and was modulated by an acoustic optical modulator (Zeiss, Germany). For time-dependent imaging of varicosities, a 40× objective (0.8 NA, Zeiss) and digitized zoom were used to collect 1–2 s (except for Fig. 3) of the individual responses in frame scan mode (~16^2 –24^2 pixels) at 33–50 Hz. Background fluorescence was corrected for the varicosity-containing regions-of-interest (ROIs) by measuring average red and green signals at regions near the dye-filled dendrite. ΔG/R was calculated as described elsewhere35. Imaging data were analyzed using custom Matlab (Math Works, Natick, MA) scripts. In Fig. 1 a correction factor of 1.05 was used to correct the ΔG/R for the differential transmission of red and green emissions in the presence of NBQX (10 μM; transmission spectra not shown).

Immunocytochemistry

For tracer injections, 50 mM of Neurobiotin (Vector Laboratories, Burlingame, CA) was added to the pipette solution. Whole-cell voltage-clamp recordings were made from A17s. Recordings were held for 20 minutes to allow Neurobiotin to diffuse into the fine dendrites. Slices were fixed in 4% paraformaldehyde for 15~20 minutes, washed with a standard solution (0.1 M phosphate buffer with 0.5% Triton X–100 and 0.1% NaN_3, pH 7.4) and blocked overnight in the standard solution with 4% donkey serum. Slices were then incubated for two hours in the standard solution containing an antibody to PKC-α (mouse, Santa Cruz Biotechnology, Santa Cruz, CA; 1:100) and an antibody to BK or BK β2 subunit (rabbit, Alomone, Jerusalem, Israel; 1:100). After extensive washing, slices were incubated for one hour in 0.1 M phosphate buffer containing Alexa-488 conjugated streptavidin (Invitrogen, Carlsbad, CA; 1:200), donkey anti–rabbit Cy3 (Jackson ImmunoResearch Laboratories, West Grove, PA; 1:200), and donkey anti–mouse Cy5 (Jackson ImmunoResearch Laboratories, West Grove, PA; 1:200). Slices were imaged using a Leica SP2 confocal microscope (Leica, Germany) with a 63× (1.32 N.A.) oil immersion objective or a Zeiss LSM–510 META confocal microscope (Zeiss) with a 100× (1.45 N.A.) oil immersion objective. For whole-mount tissues, the process was the same except the incubation period was longer (five days for the primary antibody and overnight for the secondary antibody). For quantification purposes, varicosities were defined as obvious enlargements along the A17 dendrites that were greater than or equal to twice the diameter

of the adjacent dendrite. A second criterion was the close apposition of the varicose structure to a rod bipolar terminal.

Supplementary Material

Refer to Web version on PubMed Central for supplementary material.

Acknowledgements

We thank Chris McBain for critically reading the manuscript, members of the Diamond and John Isaac laboratories for helpful discussions and Emma Compton-Daw for assistance with spectrophotometry. This work was supported by the NINDS Intramural Research Program.

References

1. Dunn FA, Doan T, Sampath AP, Rieke F. Controlling the gain of rod-mediated signals in the Mammalian retina. J Neurosci. 2006; 26:3959–3970. [PubMed: 16611812]
2. Hartveit E. Reciprocal synaptic interactions between rod bipolar cells and amacrine cells in the rat retina. J Neurophysiol. 1999; 81:2923–2936. [PubMed: 10368409]
3. Nelson R, Kolb H. A17: a broad-field amacrine cell in the rod system of the cat retina. J Neurophysiol. 1985; 54:592–614. [PubMed: 4045539]
4. Singer JH, Diamond JS. Sustained Ca2+ entry elicits transient postsynaptic currents at a retinal ribbon synapse. J Neurosci. 2003; 23:10923–10933. [PubMed: 14645488]
5. Dong CJ, Hare WA. Temporal modulation of scotopic visual signals by A17 amacrine cells in mammalian retina in vivo. J Neurophysiol. 2003; 89:2159–2166. [PubMed: 12686583]
6. Chavez AE, Singer JH, Diamond JS. Fast neurotransmitter release triggered by Ca influx through AMPA-type glutamate receptors. Nature. 2006; 443:705–708. [PubMed: 17036006]
7. Menger N, Wassle H. Morphological and physiological properties of the A17 amacrine cell of the rat retina. Vis Neurosci. 2000; 17:769–780. [PubMed: 11153656]
8. Faber ES, Delaney AJ, Sah P. SK channels regulate excitatory synaptic transmission and plasticity in the lateral amygdala. Nat Neurosci. 2005; 8:635–641. [PubMed: 15852010]
9. Hu H, et al. Presynaptic Ca2+-activated K+ channels in glutamatergic hippocampal terminals and their role in spike repolarization and regulation of transmitter release. J Neurosci. 2001; 21:9585–9597. [PubMed: 11739569]
10. Liu S, Shipley MT. Multiple conductances cooperatively regulate spontaneous bursting in mouse olfactory bulb external tufted cells. J Neurosci. 2008; 28:1625–1639. [PubMed: 18272683]
11. Maher BJ, Westbrook GL. SK channel regulation of dendritic excitability and dendrodendritic inhibition in the olfactory bulb. J Neurophysiol. 2005; 94:3743–3750. [PubMed: 16107526]
12. Ngo-Anh TJ, et al. SK channels and NMDA receptors form a Ca2+-mediated feedback loop in dendritic spines. Nat Neurosci. 2005; 8:642–649. [PubMed: 15852011]
13. Raffaelli G, Saviane C, Mohajerani MH, Pedarzani P, Cherubini E. BK potassium channels control transmitter release at CA3-CA3 synapses in the rat hippocampus. J Physiol. 2004; 557:147–157. [PubMed: 15034127]
14. Skinner LJ, et al. Contribution of BK Ca2+-activated K+ channels to auditory neurotransmission in the Guinea pig cochlea. J Neurophysiol. 2003; 90:320–332. [PubMed: 12611976]
15. Womack MD, Khodakhah K. Somatic and dendritic small-conductance calcium-activated potassium channels regulate the output of cerebellar purkinje neurons. J Neurosci. 2003; 23:2600–2607. [PubMed: 12684445]
16. Xu JW, Slaughter MM. Large-conductance calcium-activated potassium channels facilitate transmitter release in salamander rod synapse. J Neurosci. 2005; 25:7660–7668. [PubMed: 16107652]

17. Hicks GA, Marrion NV. Ca2+-dependent inactivation of large conductance Ca2+-activated K+ (BK) channels in rat hippocampal neurones produced by pore block from an associated particle. J Physiol. 1998; 508(Pt 3):721–734. [PubMed: 9518728]
18. Orio P, Rojas P, Ferreira G, Latorre R. New disguises for an old channel: MaxiK channel beta-subunits. News Physiol Sci. 2002; 17:156–161. [PubMed: 12136044]
19. Wallner M, Meera P, Toro L. Molecular basis of fast inactivation in voltage and Ca2+-activated K + channels: a transmembrane beta-subunit homolog. Proc Natl Acad Sci U S A. 1999; 96:4137–4142. [PubMed: 10097176]
20. Berkefeld H, et al. BKCa-Cav channel complexes mediate rapid and localized Ca2+-activated K+ signaling. Science. 2006; 314:615–620. [PubMed: 17068255]
21. Marty A. Ca-dependent K channels with large unitary conductance in chromaffin cell membranes. Nature. 1981; 291:497–500. [PubMed: 6262657]
22. Meredith AL, et al. BK calcium-activated potassium channels regulate circadian behavioral rhythms and pacemaker output. Nat Neurosci. 2006; 9:1041–1049. [PubMed: 16845385]
23. Sun X, Gu XQ, Haddad GG. Calcium influx via L- and N-type calcium channels activates a transient large-conductance Ca2+-activated K+ current in mouse neocortical pyramidal neurons. J Neurosci. 2003; 23:3639–3648. [PubMed: 12736335]
24. Zhang J, Li W, Trexler EB, Massey SC. Confocal analysis of reciprocal feedback at rod bipolar terminals in the rabbit retina. J Neurosci. 2002; 22:10871–10882. [PubMed: 12486181]
25. Partin KM, Patneau DK, Winters CA, Mayer ML, Buonanno A. Selective modulation of desensitization at AMPA versus kainate receptors by cyclothiazide and concanavalin A. Neuron. 1993; 11:1069–1082. [PubMed: 7506043]
26. Treiman M, Caspersen C, Christensen SB. A tool coming of age: thapsigargin as an inhibitor of sarco-endoplasmic reticulum Ca(2+)-ATPases. Trends Pharmacol Sci. 1998; 19:131–135. [PubMed: 9612087]
27. Mitra P, Slaughter MM. Mechanism of generation of spontaneous miniature outward currents (SMOCs) in retinal amacrine cells. J Gen Physiol. 2002; 119:355–372. [PubMed: 11929886]
28. Habermann CJ, O'Brien BJ, Wassle H, Protti DA. AII amacrine cells express L-type calcium channels at their output synapses. J Neurosci. 2003; 23:6904–6913. [PubMed: 12890785]
29. Ghosh KK, Haverkamp S, Wassle H. Glutamate receptors in the rod pathway of the mammalian retina. J Neurosci. 2001; 21:8636–8647. [PubMed: 11606651]
30. Euler T, Masland RH. Light-evoked responses of bipolar cells in a mammalian retina. J Neurophysiol. 2000; 83:1817–1829. [PubMed: 10758094]
31. Nelson R. AII amacrine cells quicken time course of rod signals in the cat retina. J Neurophysiol. 1982; 47:928–947. [PubMed: 6177841]
32. Wang YW, Ding JP, Xia XM, Lingle CJ. Consequences of the stoichiometry of Slo1 alpha and auxiliary beta subunits on functional properties of large-conductance Ca2+-activated K+ channels. J Neurosci. 2002; 22:1550–1561. [PubMed: 11880485]
33. Yang XL, Gao F, Wu SM. Non-linear, high-gain and sustained-to-transient signal transmission from rods to amacrine cells in dark-adapted retina of Ambystoma. J Physiol. 2002; 539:239–251. [PubMed: 11850516]
34. Ellias SA, Stevens JK. The dendritic varicosity: a mechanism for electrically isolating the dendrites of cat retinal amacrine cells? Brain Res. 1980; 196:365–372. [PubMed: 6249448]
35. Yasuda R, et al. Imaging calcium concentration dynamics in small neuronal compartments. Sci STKE. 2004; 2004:l5.

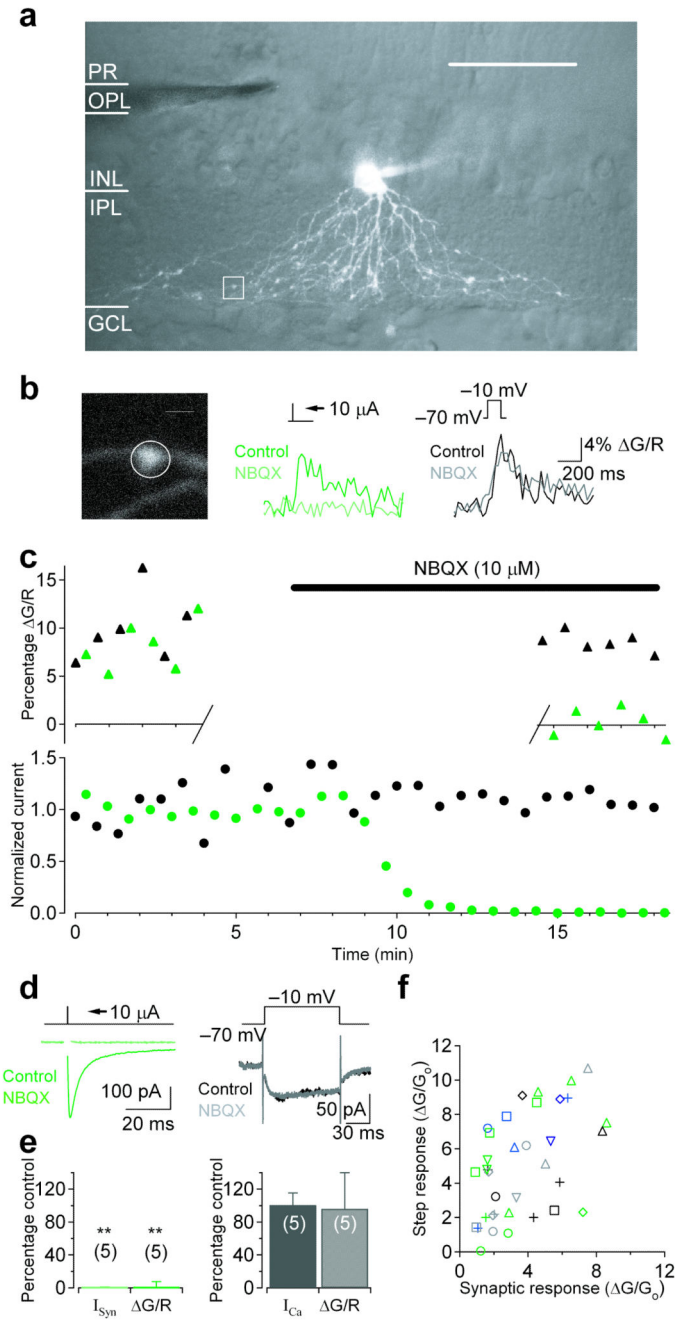

Figure 1.

Voltage-gated calcium channels are colocalized with synaptic inputs at individual A17 varicosities. (**a**–**d**) Single cell experiment. (**a**) 3D 2-photon reconstruction of an A17 amacrine cell superimposed on a single IR-DIC image of the retinal slice. Scale bar = 50 μm. (**b**) Single varicosity (left) calcium transients were observed in response to synaptic stimulation (center; green) or voltage step (right; black; −70 mV to −10 mV; 100 ms). Scale bar = 2 μm. (**c**) Fluorescence (top) and current (bottom) amplitudes plotted over time in response to interleaved stimulation (green: synaptic, black: voltage step). Application of

NBQX (10 μM) completely blocked synaptic currents and fluorescence. Single varicosity calcium fluorescence was observed for the first 12 responses (control) and for a subsequent 12 responses (NBQX) approximately 8 minutes after the onset of NBQX application to minimize photodamage. (**d**) Synaptic and voltage-dependent currents. (**e**) Summary of pharmacological effects on synaptically evoked (left) and step evoked (right) currents and fluorescence (n = 5 cells). Bar graphs indicate mean ± SD. (**f**) Varicosities exhibiting fluorescent responses to synaptic stimulation also responded to a single voltage step (35 of 36 varicosities; n = 2 cells; multiple varicosities from the same cell are indicated by identically colored/shaped symbols).

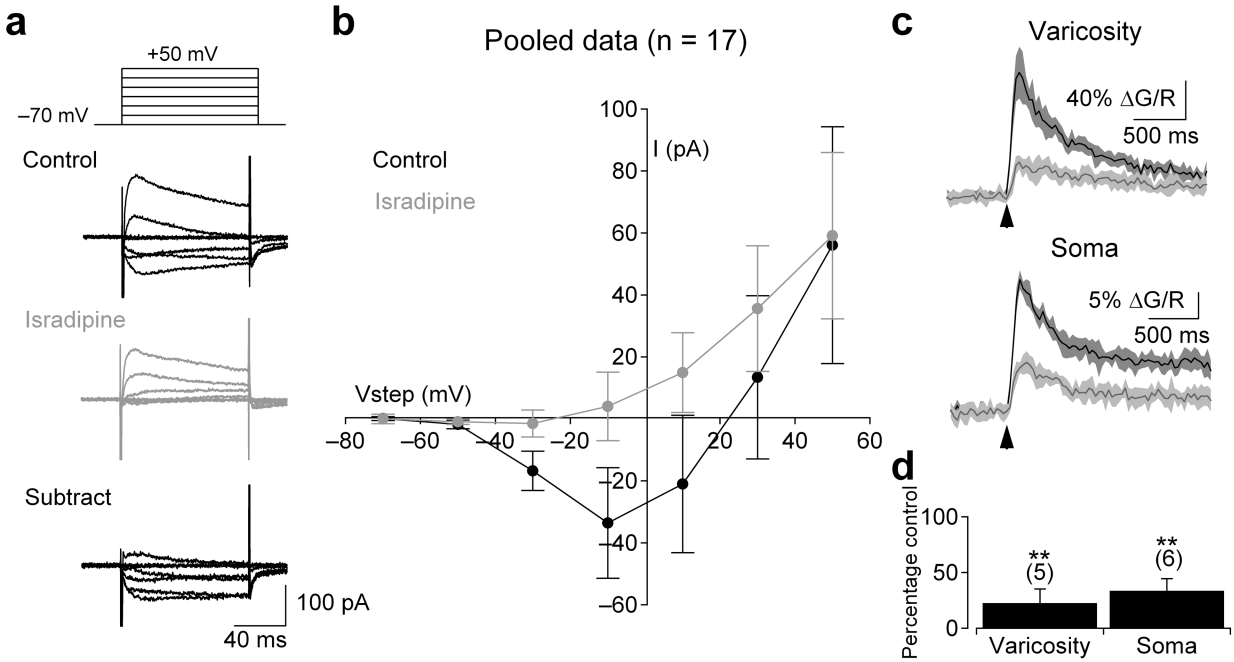

Figure 2.

Functional L-type VGCCs are expressed at A17 synaptic varicosities and somata. (**a**) A series of depolarizing voltage steps (−70 to +50 mV in 20 mV increments; 100 ms) elicited an isradipine (10 μM)- sensitive inward current. (**b**) Summary of the current-voltage relationship in control and in the presence of isradipine (10 μM; n = 17 cells). (**c**) Depolarizing voltage steps (100 ms to −10 mV) also elicited isradipine-sensitive fluorescence transients in the varicosities (top) and somas (bottom) of A17 amacrine cells. Fluorescence from a single varicosity (typically a 16×16 frame) was acquired at ~50 Hz and a small region of interest (as in Fig. 1b) was drawn around the varicosity to produce an average pixel value. Traces are the average of eight responses to 100 ms voltage steps before and after isradipine application (arrows indicate onset of step). Shaded regions indicate ± SD. (**d**) Summary of the effects of isradipine on voltage-dependent fluorescence at individual varicosities (n = 5 cells) and somas (n = 6 cells). Data in panels **b** and **d** represent mean ± SD.

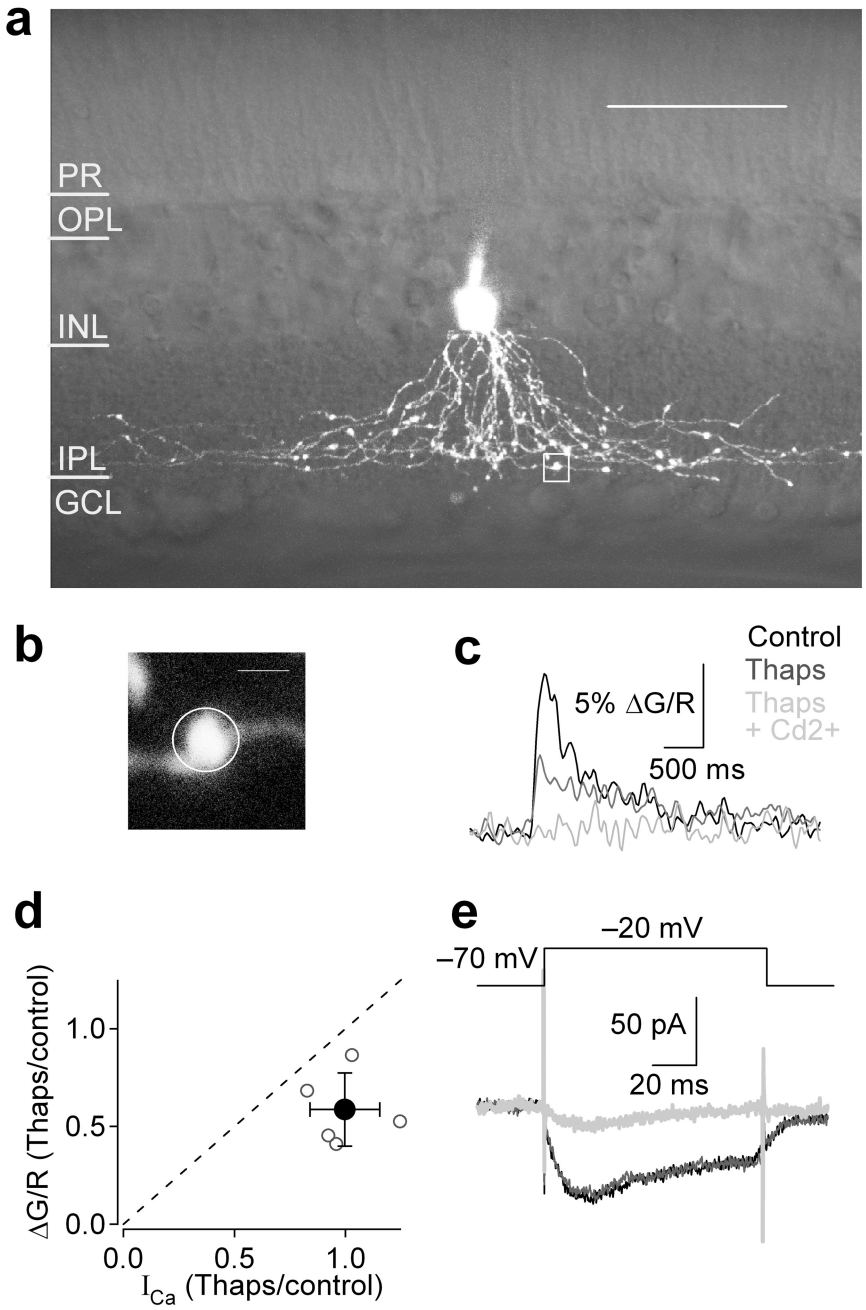

Figure 3.

Intracellular stores amplify voltage-dependent calcium responses in varicosities. (**a–c, e**) Single cell experiment. (**a**) 3D 2-photon reconstruction of an A17 amacrine cell superimposed on a single IR-DIC image of the retinal slice. Scale bar = 50 μm. (**c**) Fluorescence trace was derived from the indicated ROI (**b**, white box in **a**) in control (black), thapsigargin (1 μM; gray), and thapsigargin plus Cd^{2+} (200 μM; light gray). Scale bar = 2 μm. (**d**) Summary of the effects of thapsigargin on current and fluorescence amplitudes for 5 cells. Bar graph indicates mean ± SD. (**e**) Ca^{2+} current in control (black),

thapsigargin (gray), and thapsigargin plus Cd^{2+} (light gray). Imposed electrode potential (−70 to −20 mV; 100 ms).

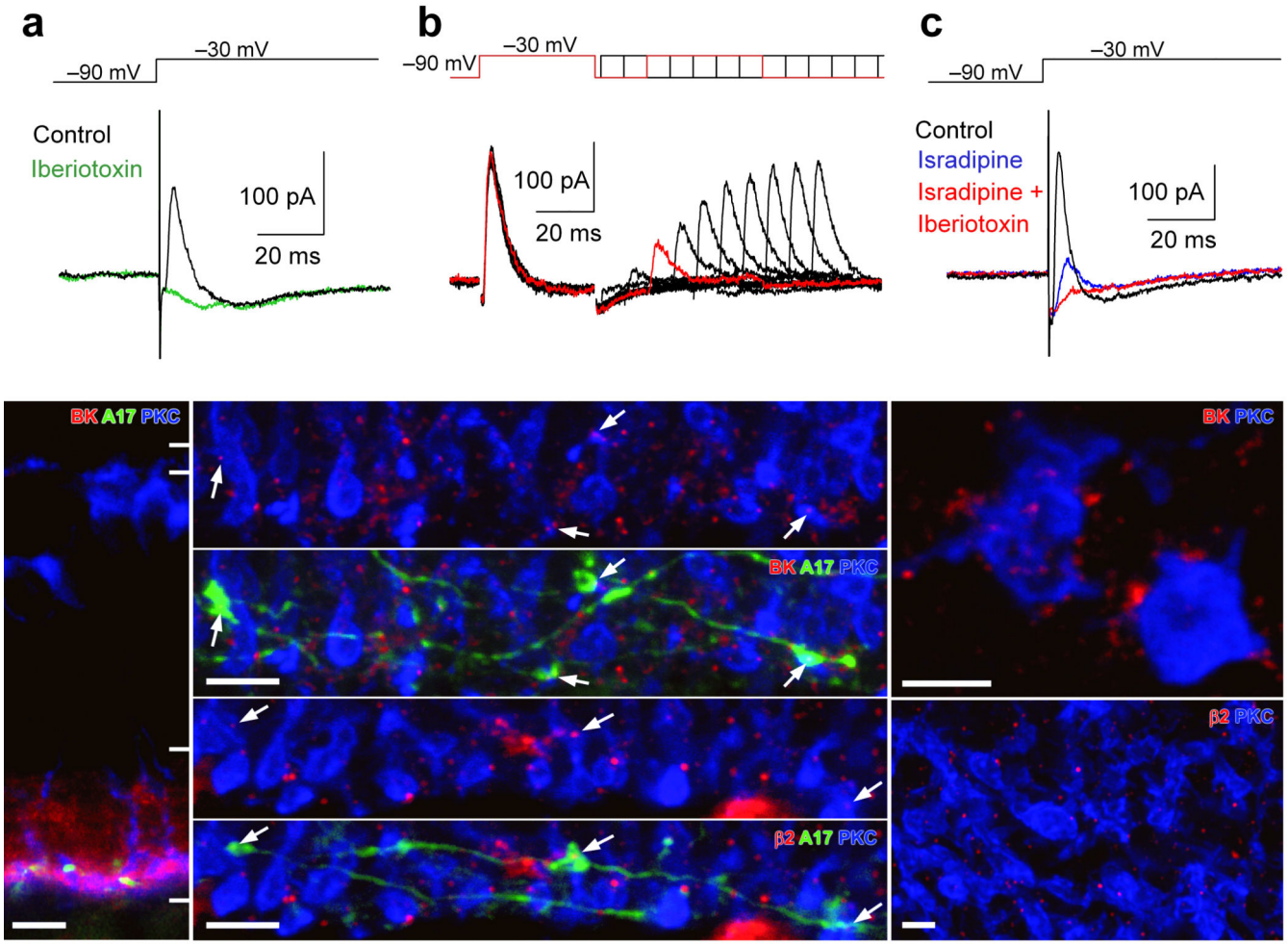

Figure 4.

A17s varicosities express rapidly inactivating BK channels that are functionally coupled to L-type VGCCs. (**a**) Depolarizing voltage steps (from −90 to −30mV; 100ms) in an A17 elicited a rapidly inactivating outward current (with potassium-based internal solution) that was blocked by iberiotoxin (100 nM) (**b**) Paired depolarizing steps delivered at varying intervals revealed the time course of recovery from inactivation. (**c**) The transient outward current also was blocked by the L-type VGCC blocker, isradipine (10 μM). (**d**) Immunohistochemical techniques reveal BK (red) channel expression throughout the inner plexiform layer of a slice. Anti-PKCα was used to label RBCs (blue) and the dendrites of a single A17 were filled with neurobiotin (green) through the patch pipette. Scale bar = 10 μm. (**e,f**) A higher-magnification view of sublamina 5 in the IPL indicates that BK (**e**) and β2 subunit (**f**) puncta are localized to A17 varicosities that are adjacent to RBC terminals. Scale bars = 5 μm. (**g,h**) Antibody staining for PKC (blue) and BK (red, **g**) or β2 (red, **h**) in whole-mount retina illustrates the clustering of channels antibody around RBC terminals. Scale bars = 2 μm.

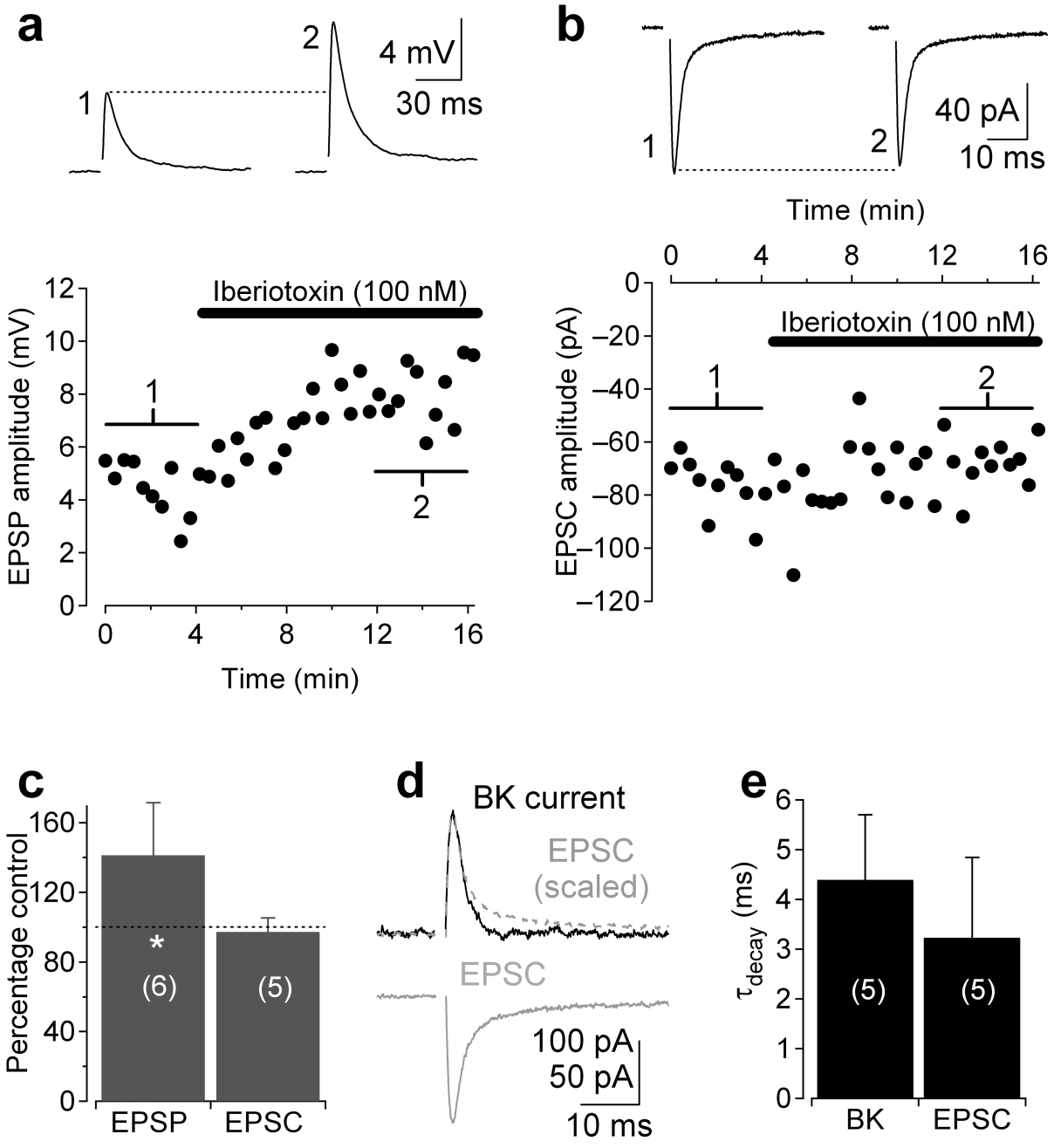

Figure 5.

BK channels suppress synaptic transmission. (**a**) Synaptic stimulation of current-clamped A17 elicited EPSPs which were potentiated by application of iberiotoxin (black bar, 100 nM). (**b**) EPSCs (in Cs-based internal) were recorded from A17 in control and iberiotoxin to test for possible presynaptic effects of the BK channel antagonist. Traces in **a** and **b** are averages of 10 responses centered around corresponding numbers in the diary plot. (**c**) Pooled data from experiments in **a** and **b**. (**d**) Voltage-activated BK current (black) AMPAR-mediated EPSC (gray) from the same cell superimposed to demonstrate the

similarity in kinetics. *Gray dashed trace*, EPSC inverted and scaled to the same amplitude as the BK current. (**e**) Pooled data comparing the time course of BK inactivation and EPSC decay across cells. Data in panels **c** and **e** represent mean ± SD.

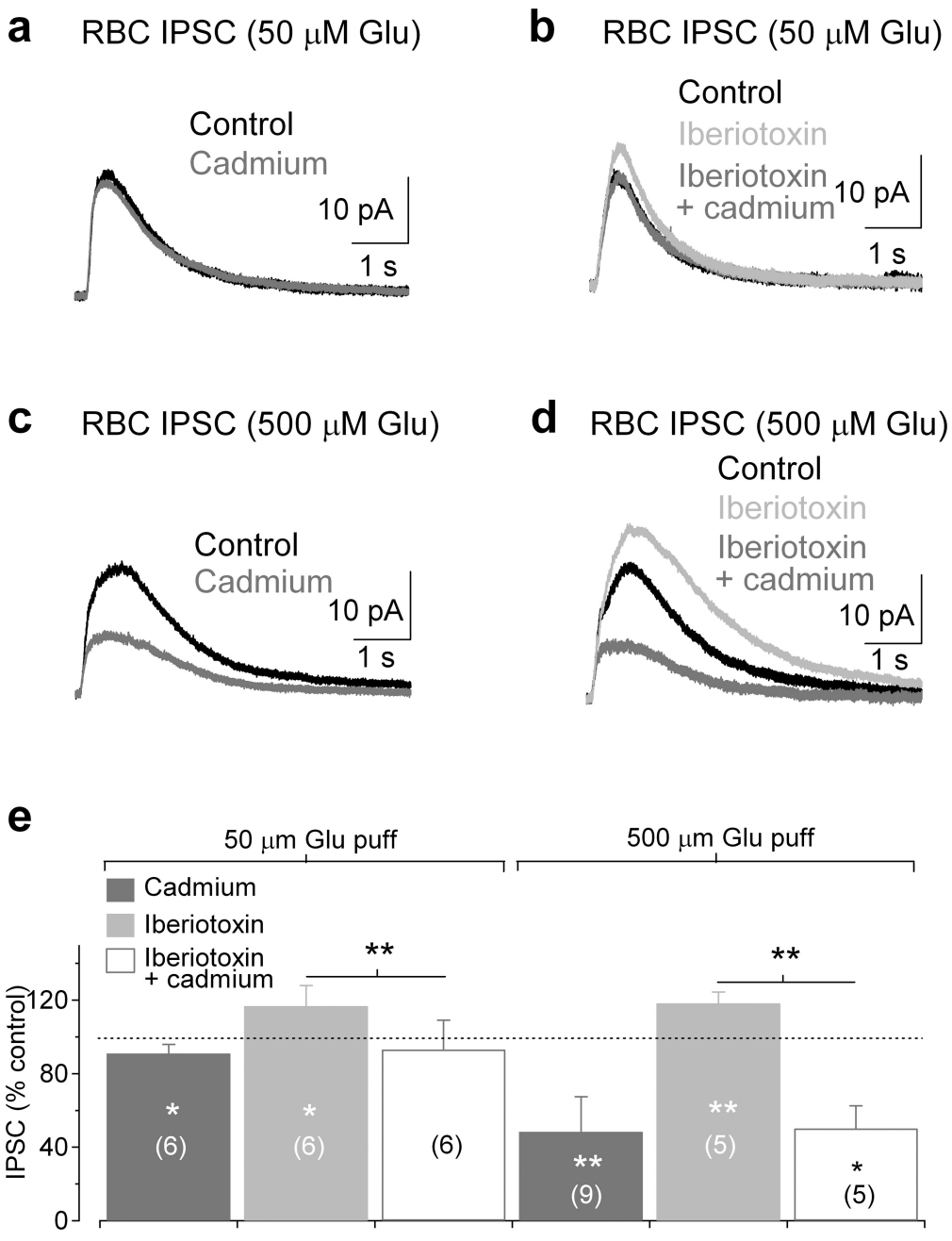

Figure 6.

BK channel-modulated Ca_v channels enhance GABA release from A17s. (**a**) Puffing 50 μM glutamate (25 ms) onto A17 dendrites elicited IPSCs in RBCs that were only minimally sensitive to the divalent Ca_v channel blocker Cd^{2+} (200 μM). (**b**) Blocking BK channels with iberiotoxin (100 nM) enhanced IPSCs (50 μM puff) and increased Cd^{2+} sensitivity. (**c**) Increasing the glutamate puff concentration (500 μM) elicited RBC IPSCs that were sensitive to Cd^{2+}, providing evidence that Ca_v channels contribute to GABA release. (**d**) Application of iberiotoxin enhanced the IPSCs (500 μM puff) and increased the Cd^{2+}

sensitivity of the response. (**e**) Summary of the results from experiments in **a**–**d**. Bar graph indicates mean ± SD.

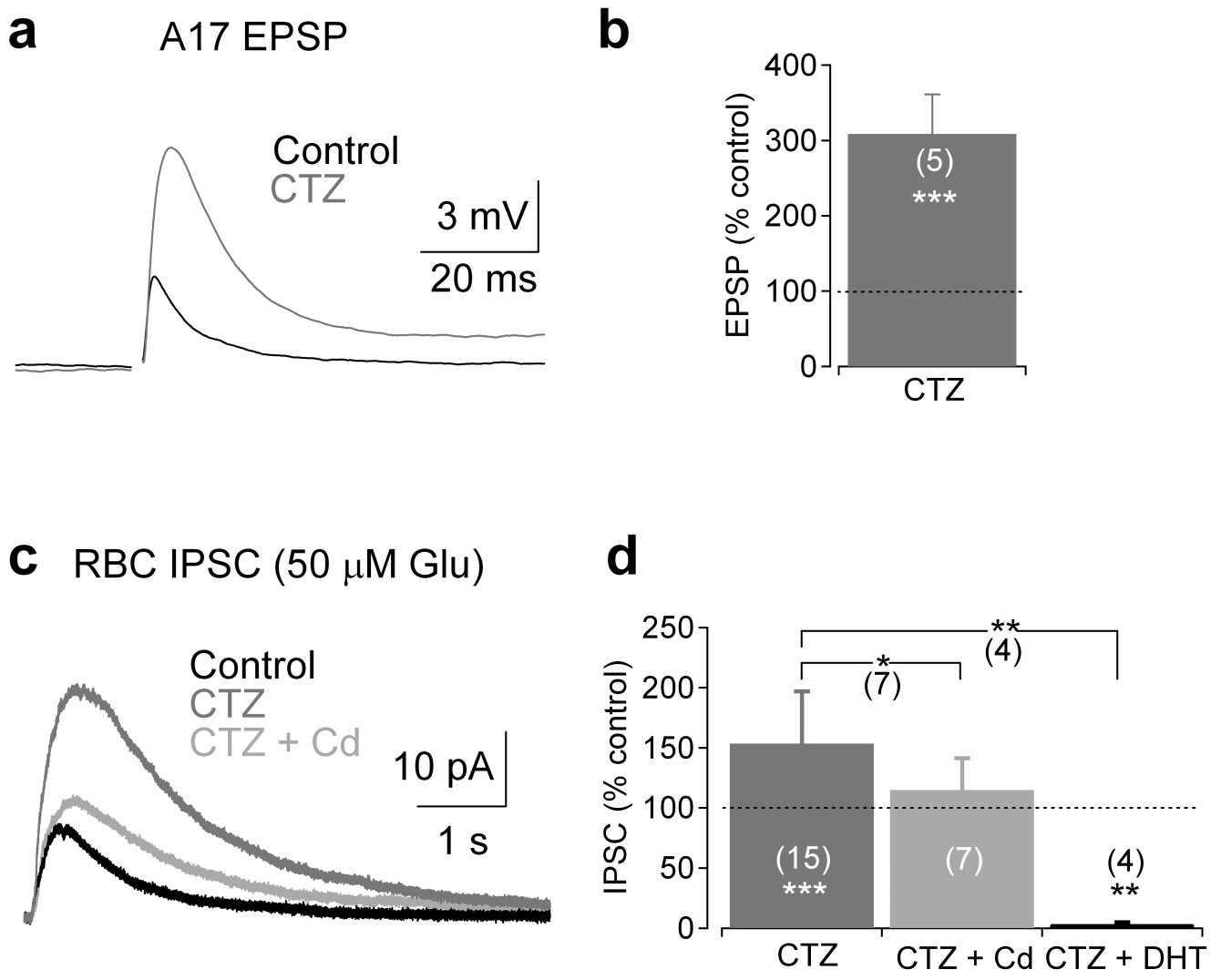

Figure 7.

Modification of AMPAR kinetics with cyclothiazide recruits Ca_V channel-dependent enhancement of GABA release. (**a**) Electrically-evoked A17 EPSPs were strongly potentiated by cyclothiazide. (**b**) Summary of results from experiments described in **a**. (**c**) RBC IPSCs evoked by 50 μM glutamate puff were strongly enhanced by cyclothiazide application (50 μM). Cyclothiazide-enhanced IPSCs were reduced by Cd^{2+} (200 μM) application or abolished by the toxic serotonin analog DHT (50 μM; example trace not shown). (**d**) Summary of results from the experiment described in **c**. Bar graph indicates mean ± SD

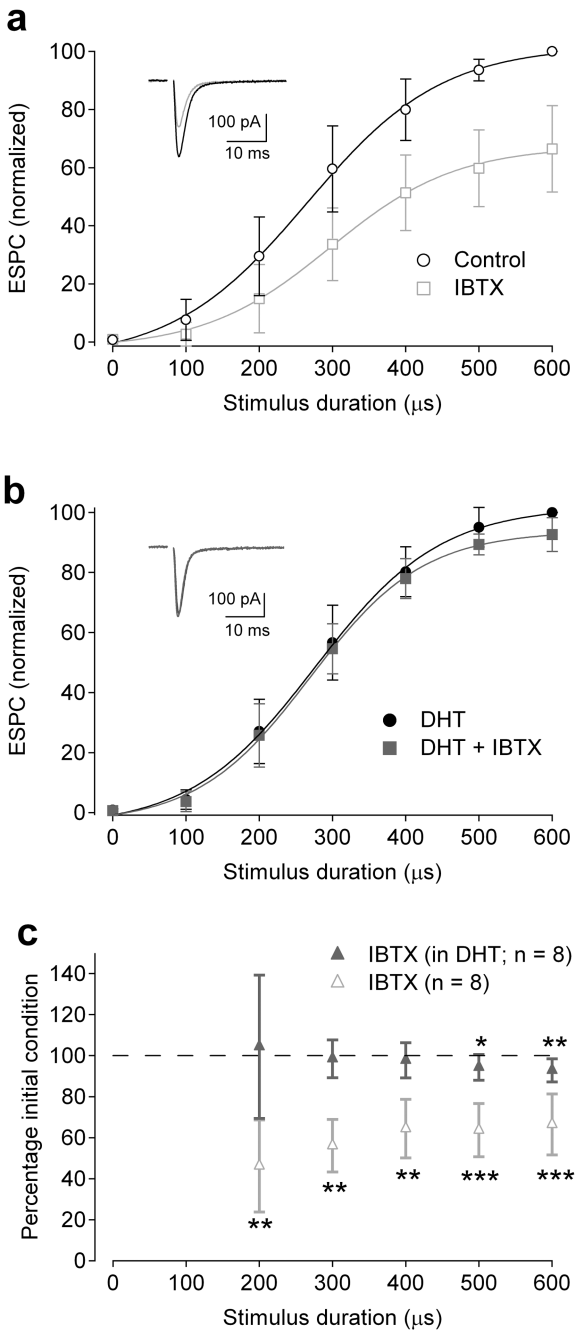

Figure 8.

BK channels in A17 amacrine cells modulate feedforward excitatory signaling at the RBC dyad. (**a**) EPSCs recorded in AII amacrine cells, reflecting synaptic output from RBCs, were reduced by iberiotoxin (IBTX, 100 nM; n = 8). *Inset*, Representative responses to 300 μs stimulation in control conditions (black) and the presence of iberiotoxin. (**b**) When A17s were ablated with 5,7-DHT, the BK channel-dependent modulation was strongly reduced. (**b** *inset*) Representative responses to 300 μs stimulation in the presence of 5,7-DHT (black) and with the addition of iberiotoxin (red; IBTX, 100 nM). (**c**) Summary of data in **a** and **b**,

showing that iberiotoxin affected feedforward signaling when A17 amacrine cell feedback was intact. Data is represented as mean ± SD